# Cold-welding fabrication of highly ordered gold nanochannel monolayers in aqueous medium†

**Yingpu Bi and Jinhua Ye***

*Received 29th June 2010, Accepted 27th July 2010*
**DOI: 10.1039/c0cc02178d**



**Herein, we demonstrate that galvanic replacement reaction over aligned Ag nanowire arrays can be employed as a simple and powerful cold-welding technique for large-scale fabrication of highly ordered Au nanochannel monolayers.**

One-dimensional (1D) metal nanostructures, such as nanowires and nanotubes, have attracted intense interest due to their great potential in fabricating nanoscale electronics, optoelectronics, and molecular sensing devices for practical applications.[1–5] However, one of the most significant challenges still facing devices fabrication and processing is how to join these individual 1D building blocks together by strong metallic bonds to ensure the longer lifetimes of nano-devices. In an attempt to address this issue, many localized welding methods have recently been proposed, including thermal heating,[6] ion beam deposition,[7] laser heating,[8] ultrasonic irradiation,[9] high-energy electron beam bombardment,[10] and Joule heating.[11,12] Although these novel methods have greatly expanded our ability to construct a wide range of devices at the nanoscale, it is worth pointing out that there are some limitations still inherent in the present fabrication processes. For example, such nanoscale welding techniques have always involved local heating processes,[13,14] which make it difficult to achieve precise weld control and may increase the possibility of damage to the original metal building blocks. Moreover, they usually require special apparatus, rigorous conditions, and complex operating processes, which greatly restricts their future practical applications.

Herein, we demonstrate, for the first time, that galvanic replacement reaction over well-aligned Ag nanowire arrays can be employed as a simple and powerful cold-welding technique for large-scale fabrication of highly ordered Au nanochannel monolayers at room temperature. Additionally, the aspect ratios of Au monolayers can be rationally tailored by adjusting the number of Ag nanowires in the assembly, and different shaped Au nanostructures such as nanochannels and nanocups can also be welded together.

Fig. 1A and Fig. S1 show typical scanning electron microscopy (SEM) images of silver nanowire arrays synthesized by a simple water processing strategy.[15] It is found that these nanoarrays exhibit well-defined long-range parallel architectures, and all the nanowires are directly attached with their two opposite {100} facets (inset in Fig. 1A and Fig. S2), resembling

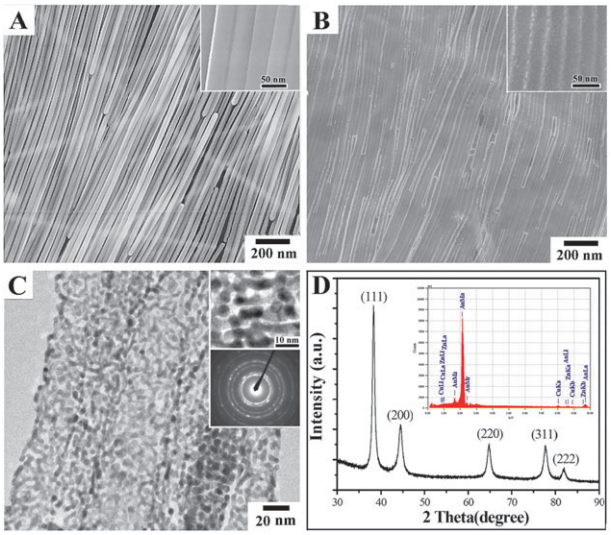


**Fig. 1** (A) SEM images of Ag nanowires array, (B) SEM images, (C) TEM images, and (D) XRD and EDS pattern of Au nanochannel monolayer.

a 2D ordering monolayer. Fig. 1B and Fig. S3 show the SEM images of gold products that were fabricated by reacting above Ag nanowire arrays with $HAuCl_4$ in saturated NaI aqueous solutions at room temperature. Interestingly, a novel 2D nanostructure, nanochannel monolayer, has been fabricated over a large area by this modified replacement process. The enlarged SEM images (inset in Fig. 1B and Fig. S3D) clearly indicate that these Au nanochannels possess a unique concave cross section and smooth inner surfaces, which serve as the building blocks to be welded together into horizontally aligned monolayer structures with corrugated surfaces. Furthermore, their crystalline structures and morphologies have been further clarified by transmission electron microscopy (TEM) and electron diffraction (ED). As shown in Fig. 1C, these Au nanochannel monolayers exhibit parallel and interconnected planar structures, and their longitudinal junctions were joined by the networked Au nanocrystals with average diameters of 5–7 nm. Moreover, their ED pattern shows that all diffraction rings could be assigned to face-centre-cubic (fcc) gold crystals, indicating the polycrystalline structure of as-synthesized Au monolayers. The X-ray diffraction (XRD) pattern (Fig. 1D) gives further support to the above ED results, and all the diffraction peaks could be indexed to the (111), (200), (220), (311), and (222) planes of gold (PCPDF No. 04-0784), respectively. Additionally, the energy dispersive spectroscopy (EDS) pattern (inset in Fig. 1D) clearly shows that no diffraction peak corresponding to Ag or other impurities has been detected, indicating that this modified replacement

*International Center for Materials Nanoarchitectonics (MANA), and Photocatalytic Materials Center, National Institute for Materials Science (NIMS), 1-2-1 Sengen, Tsukuba, Ibaraki 305-0047, Japan. E-mail: jinhua.ye@nims.go.jp*

† Electronic supplementary information (ESI) available: Experimental procedure and additional figures. See DOI: 10.1039/c0cc02178d

 

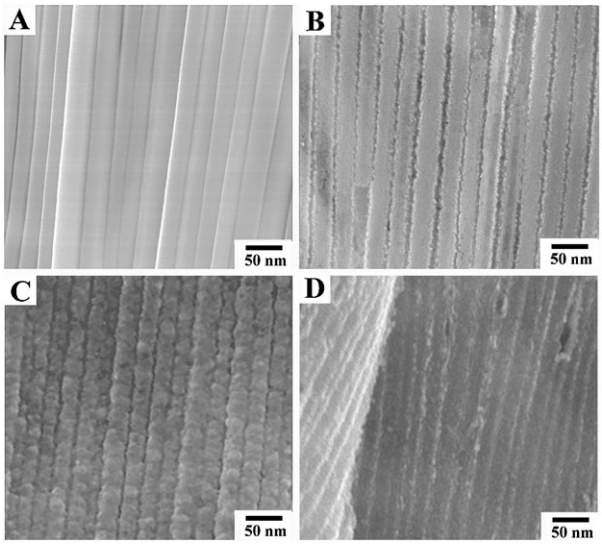


**Fig. 2** (A–D) SEM images of the Ag nanowire monolayer titrated with different amounts of 0.02 M $HAuCl_4$. (A) 0 mL; (B) 1 mL; (C) 2 mL; (D) 3 mL.

reaction could proceed completely and the final product is only composed of pure gold.

Fig. 2 and Fig. S4, S5 summarize all major morphological and composition changes of the samples involved in this novel welding process. As shown in Fig. 2B and Fig. S4B, when the close-packed and ordered rectangular Ag nanowire arrays (Fig. 2A) were mixed with aqueous $HAuCl_4$ solutions, the replacement reaction between Ag and $AuCl_4^-$ ions occurred immediately. More specifically, the reaction was initiated from the side edges of Ag nanowires through a pitting process because they possess higher surface energies (Fig. 2B), and hollow Au/Ag aligned nanotube arrays have been formed at this stage. Furthermore, it should be noted that these alloy nanotubes still inherited the aligned arrangements of the original Ag nanowire arrays, indicating the strong attachment between proximal Ag nanowires preventing disassembly during the replacement process. As the reaction proceeded, Au atoms were deposited on the whole surface of Ag nanocrystals including the junctions of Ag nanowires, through a combination of replacement and dealloying process between Ag and Au, promoting the welding formation of plate-like nanostructure (Fig. 2C). Note that these close-packed {100} facets have been selectively etched and dissolved, which leads to the formation of Au products with wholly hollow interiors. Owing to the novel structures, these Au products could easily separate into two individual nanochannel monolayers (Fig. 2D). Finally, Au nanochannel monolayers with a highly ordered and aligned structure evolved as a result of the Ostwald ripening process.

To further help understand the above *in situ* welding process, we identified a schematic illustration showing the potential replacement mechanism between Ag nanowire arrays and $HAuCl_4$ solution (Scheme 1). Furthermore, a key feature of the successful welding fabrication of Au monolayers with high quality could be attributed to the use of highly ordered and aligned Ag nanowire arrays as the sacrificial templates. More specifically, these rectangular Ag nanowires

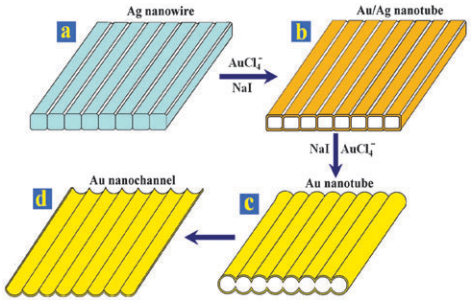


**Scheme 1** Schematic illustration of the replacement process between Ag nanowire arrays and $HAuCl_4$ in saturated NaI solutions.

were directly attached to each other with their {100} facets in the assembly, which leads to the formation of well-defined interface contacts with tiny interspaces, thus affording a perfect template for the subsequent welding process. Additionally, these Ag nanowire arrays may serve as anisotropic ultra-thin films for the replacement reaction with $AuCl_4^-$, which leads to significant changes in the electron transport rates between Ag and Au and deposition growth of Au atoms. For example, when random and individual Ag nanowires were also introduced in this replacement system, only commonly hollow tubular structures were synthesized (Fig. S6).

In addition to large-scale fabrication, this process can also be adapted to the precise welding of Au nanostructures within a small range. As shown in Fig. S7 and Fig. 3, when only two aligned Ag nanowires were used as the starting materials, the dimers of Au nanochannels were routinely synthesized. Moreover, except for Ag nanowires having the same crystal orientation and structure, the welds could be performed between dissimilarly shaped Ag nanocrystals. As shown in Fig. 3C and D, the Ag nanoparticles were transformed into Au nanocups that were inlaid between two Au nanochannels to construct a sandwich-like structure. These demonstrations clearly indicate that the successful welding of aligned Au nanostructures is independent of the morphology and numbers of Ag nanocrystals, and the only requirement is their direct interface contacts, which may offer a facile and general process for welding fabrication of complex nanostructures.

Furthermore, we speculate that saturated NaI solutions should also play multiple roles in the successful welding fabrication of Au nanochannel monolayers in this system.[16] First of all, $I^-$ ions with a high concentration could react with the generated silver halides to form the soluble complex of

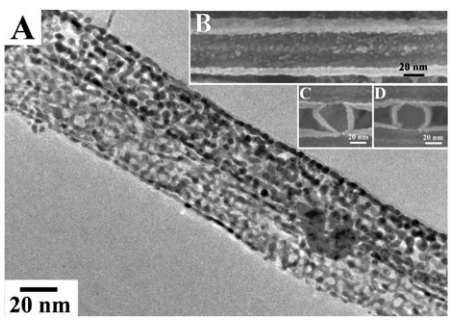


**Fig. 3** (A) TEM and (B) SEM images of Au nanochannel dimer; (C,D) SEM images of Au nanochannel and nanocup complexes.

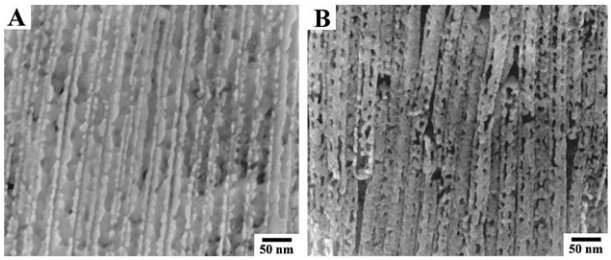


**Fig. 4** SEM images of Au nanoproducts prepared in (A) saturated NaBr aqueous solutions, (B) saturated NaCl aqueous solutions.

$[AgI_3]^{2-}$,[17] which makes the replacement reaction between Ag and $AuCl_4^-$ occur completely and results in Au products with pure composition. Second, with the help of $I^-$ ions, the redox potential of Ag species has been decreased markedly from +0.80 V ($Ag^+/Ag$ *vs.* SHE) to −0.15 V (AgI/Ag), thereby the rapid electron transport between Ag and $AuCl_4^-$ has been achieved, which makes it possible to quickly weld individual products together into an integrated structure. Third, owing to its low redox potential ($E^{\ominus}_{I/I^-}$ = 0.535 V), $I^-$ ions can serve as additional reducing agent to reduce $AuCl_4^-$ into Au crystals ($E^{\ominus}_{Au/AuCl_4^-}$ = 0.993 V), which may prevent the collapse of final products into tiny fragments as reported by Xia *et al.*[18] To further confirm the above hypothesis, the morphology and structure evolutions of Au products fabricated in other sodium halide solutions have also been studied. As shown in Fig. 4A, when NaI was replaced by NaBr, the as-synthesized Au products also exhibit monolayer structures, while some large interspaces between the neighboring nanochannels have been observed. Additionally, in the presence of NaCl solution, only noncompact hollow Au nanotubes with poor structures have been synthesized, and no welds could be achieved in this reaction system (Fig. 4B). Thus, it appears that the $I^-$ ions are essential for the successful welding of Au nanochannel monolayers. More specifically, these changes could be attributed to the increases in the redox potentials of silver couples ($E^{\ominus}_{AgBr/Ag}$ = 0.007 V, $E^{\ominus}_{AgCl/Ag}$ = 0.223 V) and non-reducibility of both $Br^-$ and $Cl^-$ ions for $AuCl_4^-$ ions ($E^{\ominus}_{Br_2/Br^-}$ = 1.087 V, $E^{\ominus}_{Cl_2/Cl^-}$ = 1.358 V).

Finally, the electrochemical performances of as-synthesized Au monolayers were explored for HCHO oxidation in alkaline solution to investigate their potential applications.[19] As shown in Fig. 5, these Au nanochannel monolayers exhibit excellent electrocatalytic activity towards this reaction. More specifically, with increasing HCHO amounts from 0.13 to 1.69 mM, the peak current densities of the Au nanochannel monolayer electrode increased from 1.64 up to 15.11 mA $cm^{-2}$ (Fig. 5A). Additionally, a good linear relationship between HCHO amounts and current densities has been summarized in Fig. 5B, clearly indicating that this Au monolayer-based electrocatalytic reaction could also serve as an alternative highly sensitive method for rapid HCHO detection. Moreover, the electrocatalytic properties of Au nanoparticles and commercial bulk Au electrode under the same conditions have also been studied and compared in Fig. S8. It can be clearly seen that these novel Au monolayers exhibit much higher electrocatalytic activities, which may be due to their novel anisotropic 2D nanostructure with high aspect ratios that can

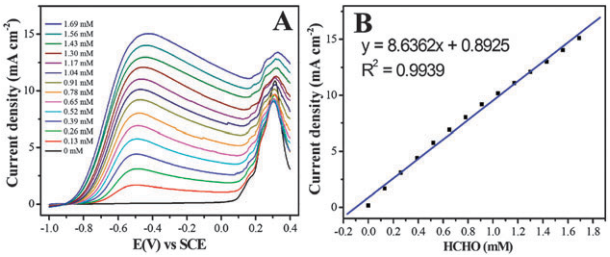


**Fig. 5** (A) Electrocatalytic activity of Au nanochannel monolayer for HCHO oxidation in 1.0 M KOH with scan rate 50 mV $s^{-1}$. (B) The relationship between peak current densities and HCHO concentrations.

effectively improve mass transport and catalyst utilization for this oxidation reaction. More detailed investigation on their electrocatalytic mechanisms is still in progress.

In summary, we have demonstrated a simple and powerful cold-welding process for fabricating aligned Au nanochannel monolayers based on the replacement reaction between rectangular Ag nanowire arrays and $HAuCl_4$ at room temperature. This study clearly reveals that replacements and welds can be perfectly combined in a single-step procedure for finer joining of Au nanomaterials.

## Notes and references


1 F. Patolsky, Y. Weizmann and I. Willner, *Nat. Mater.*, 2004, **3**, 692.
2 L. Liu, S. Yoo and S. Park, *Chem. Mater.*, 2010, **22**, 2681.
3 Y. Chen, S. Milenkovic and A. W. Hassel, *Nano Lett.*, 2008, **8**, 737.
4 Z. Liu, S. Li, Y. Yang, S. Peng, Z. Hu and Y. Qian, *Adv. Mater.*, 2003, **15**, 1946.
5 (*a*) X. Fang, Y. Bando, U. Gautam, C. Ye and D. Golberg, *J. Mater. Chem.*, 2008, **18**, 509; (*b*) J. Fei, Y. Cui, A. Wang, P. Zhu and J. Li, *Chem. Commun.*, 2010, **46**, 2310; (*c*) T. Olson and J. Zhang, *J. Mater. Sci. Technol.*, 2008, **24**, 433; (*d*) X. Fang, Y. Bando, M. Liao, U. Gautam, C. Zhi, B. Dierre, B. Liu, T. Zhai, T. Sekiguchi, Y. Koide and D. Golberg, *Adv. Mater.*, 2009, **21**, 2034.
6 Z. Y. Gu, H. K. Ye and D. H. Gracias, *JOM*, 2005, **57**, 60.
7 S. Matsui, T. Kaito, J. Fujita, M. Komuro, K. Kanda and Y. J. Haruyama, *J. Vac. Sci. Technol., B*, 2000, **18**, 3181.
8 J. C. She, S. An, S. Z. Deng, J. Chen, Z. M. Xiao, J. Zhou and N. S. Xu, *Appl. Phys. Lett.*, 2007, **90**, 73103.
9 C. Chen, L. Yan, E. Kong and Y. Zhang, *Nanotechnology*, 2006, **17**, 2192.
10 S. Y. Xu, M. L. Tian, J. G. Wang, H. Xu, J. M. Redwing and M. H. W. Chan, *Small*, 2005, **1**, 1221.
11 H. Tohmyoh, T. Imaizumi, H. Hayashi and M. Saka, *Scr. Mater.*, 2007, **57**, 953.
12 Y. Peng, T. Cullis and B. Inkson, *Nano Lett.*, 2009, **9**, 91.
13 S. H. Christiansen, M. Becker, S. Fahlbusch, J. Michler, V. Sivakov, G. Andra and R. Geiger, *Nanotechnology*, 2007, **18**, 035503.
14 Y. Lu, J. Y. Huang, C. Wang, S. Sun and J. Lou, *Nat. Nanotechnol.*, 2010, **5**, 218.
15 Y. Bi, H. Hu and G. Lu, *Chem. Commun.*, 2010, **46**, 598.
16 (*a*) A. Pearson, A. Mullane, V. Bansal and S. Bhargava, *Chem. Commun.*, 2010, **46**, 731; (*b*) Y. Bi and J. Ye, *Chem. Commun.*, 2010, **46**, 1532.
17 C. H. Gammons and Y. Yu, *Chem. Geol.*, 1997, **137**, 155.
18 Y. Sun, B. Mayers and Y. Xia, *Adv. Mater.*, 2003, **15**, 641.
19 (*a*) Y. Suo, L. Zhuang and J. Lu, *Angew. Chem., Int. Ed.*, 2007, **46**, 2862; (*b*) D. Zhao, B. Yan and B. Xu, *Electrochem. Commun.*, 2008, **10**, 884; (*c*) P. Wang, B. Huang, X. Qin, X. Zhang, Y. Dai, J. Wei and M. Whangbo, *Angew. Chem., Int. Ed.*, 2008, **47**, 7931.


 